High-temperature order-disorder transition and polaronic conductivity in $PrBaCo_2O_{5.48}$

S. Streule,[1,*] A. Podlesnyak,[1] D. Sheptyakov,[1] E. Pomjakushina,[2,1] M. Stingaciu,[2,1] K. Conder,[2] M. Medarde,[2,1] M. V. Patrakeev,[3] I. A. Leonidov,[3] V. L. Kozhevnikov,[3] and J. Mesot[1]

[1]*Laboratory for Neutron Scattering, ETH Zürich & Paul Scherrer Institut, CH-5232 Villigen PSI, Switzerland*

[2]*Laboratory for Developments and Methods, Paul Scherrer Institut, CH-5232 Villigen PSI, Switzerland*

[3]*Institute of Solid State Chemistry RAS, Ekaterinburg 620219, Russia*

(Received 19 January 2006; published 24 March 2006)

Neutron powder diffraction and transport measurements have been used to investigate the $PrBaCo_2O_{5.48}$ compound between room temperature and 820 K. A structural phase transition, involving a rearrangement of oxygen vacancies, was found at $T_{OD}=776$ K. Across the transition the perovskite structure loses its vacancy ordering, and the crystal symmetry changes from orthorhombic *Pmmm* to tetragonal *P4/mmm*. The resisitivity measurements for temperatures above ~350 K yield high values of ρ, indicating that the compound is rather semiconducting than metallic as usually accepted. A model in terms of thermally activated hole (polaronic) hopping is proposed.

DOI: 10.1103/PhysRevB.73.094203 PACS number(s): 61.12.Ld, 72.80.Ga

Transition metal oxides with perovskite structure display a wide variety of fascinating properties. Among the most prominent examples are superconductivity occurring in cuprates and colossal magnetoresistivity in manganites. These materials, whose crystal structures consist of simple metal-oxygen planes, show intriguing phase diagrams, which include complicated magnetic and structural phase transitions, and charge and orbital ordering. An additional degree of freedom is found in Fe and Co ions since, depending on the ratio of the crystal field and intra-atomic exchange energies, they can adopt up to three different spin states. The energy difference between them is small and can be tuned, by changing temperature or pressure.[1–3] The layered cobaltites $RBaCo_2O_{5+\delta}$ (R=rare−earth, $0\leqslant\delta\leqslant 1$) have received particular attention[4–9] due to the discovery of giant magnetoresistivity in the materials with $\delta=0.4$, R=Er, Gd.[5,10] Materials with $\delta=0.5$ show a change in resistivity in the temperature range $300\ \mathrm{K}<T<350\ \mathrm{K}$ depending on the rare earth R.[5] Although this transition is usually associated to a spin-state change of the Co^{3+} ion on the octahedral site,[4–6,10–13] the underlying mechanism for the spin-state crossover is still under debate.

At high temperatures cobaltites are furthermore interesting for their high ionic conductivity, thus showing potential for applications as gas sensors, oxidation catalysts, or materials for fuel cells. Ionic conductivity in cobaltites was first observed in 1991 by Teraoka[14] in $La_{0.6}Sr_{0.4}Co_{0.8}B_{0.2}O_{3-\delta}$ (B=Fe, Co, Ni, Cu) and it is believed that oxygen order-disorder phenomena play an important role for its occurrence.[15–19]

Since no information exists about the high-temperature structures of layered cobaltites, we decided to investigate $PrBaCo_2O_{5.48}$ by means of neutron powder diffraction (NPD). This is a powerful technique for structure determination, which provides reliable infomation on the oxygen ion positions and occupancies. Transport measurements were performed to detect possible changes in the electronic properties of the sample in the investigated temperature range.

The $PrBaCo_2O_{5+\delta}$ sample was synthesized by the solid state reaction method and its oxygen content adjusted as described previously.[20] The oxygen content was determined to be 5.48 ± 0.01 by iodometric titration.[21] We have checked by thermogravimetry in inert atmosphere, that there is no mass change of the sample up to 825 K. This ensures constant oxygen content within the whole temperature range of our NPD measurements. Phase purity was checked with a conventional x-ray powder diffractometer (Cu $K\alpha$ radiation) and differential scanning calorimetry (DSC) was used to detect possible phase transitions. dc resistivity and thermoelectric power were measured in He atmosphere (300–830 K) by the four-probe method on a bar-shaped $2\times2\times15\ \mathrm{mm}^3$ ceramic sample.[22] Coulometric titration[23] was used to determine the equilibrium oxygen content in $PrBaCo_2O_{5+\delta}$ $0.16\leqslant\delta\leqslant0.76$ cobaltites at different values of temperature and partial oxygen pressure. The neutron powder diffraction measurements were carried out on the high resolution diffractometer HRPT (Ref. 24) at SINQ (PSI, Switzerland) in the angular range $7\ \mathrm{deg}<2\Theta<165$ deg and temperature range $300\ \mathrm{K}\leqslant T\leqslant820\ \mathrm{K}$, using two wavelengths $\lambda=1.494$ and 1.889 Å. The sample holder was made out of steel and tightly sealed under helium atmosphere. Our NPD data were refined using the program FULLPROF.[25]

We now turn to the description of our data (based on NPD measurements using $\lambda=1.494$ Å, unless otherwise indicated). We find that for $T\leqslant780$ K the crystal structure can be refined using the orthorhombic *Pmmm* space group.[5,6,26] In this model (Fig. 1) the simple cubic perovskite cell is doubled along the c axis due to the ordering of Pr and Ba ions and along the b axis due to ordering of oxygen vacancies (unit cell $a_p\times2a_p\times2a_p$, with a_p the cubic lattice constant). The oxygen site O4 has been found to be almost empty, while the O3 site is nearly fully occupied, see Table I. This results in planes of CoO_6 octahedra and CoO_5 pyramids parallel to the ac planes, which alternate along the b direction. The oxygen occupancy was refined for the positions O3 and O4 (Table I). The anisotropic B factor was restrained to be the same for Co1/Co2, as well as for O1/O2/O3/O4 and O5/O6. Refined structural parameters, occupancies, χ^2 and

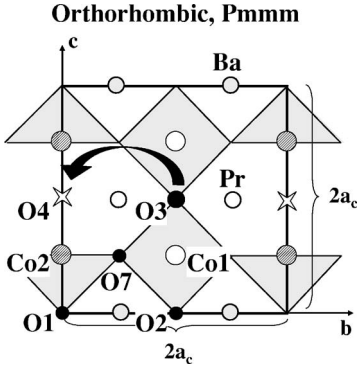

FIG. 1. Schematic view of the $PrBaCo_2O_{5.48}$ structure in the *bc* plane. For clarity only O1, O2, O3, O4, and O7 sites are shown and the arrow indicates the high temperature rearrangement of oxygen.

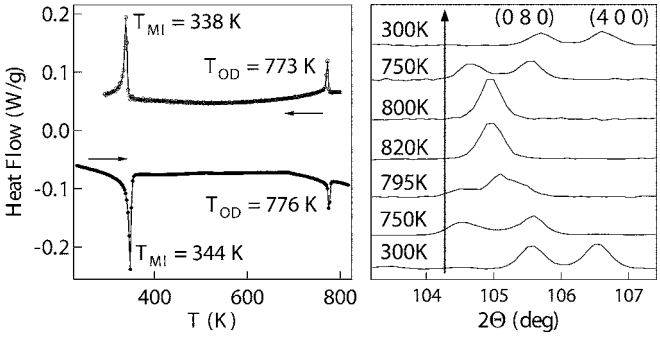

FIG. 2. Left: DSC measurement for $PrBaCo_2O_{5.48}$. Right: temperature dependent evolution of the (0 8 0) and (4 0 0) reflections upon heating and cooling (bottom to top, orthorhombic notation). Measured with $\lambda = 1.889$ Å.

R_{Bragg} values for representative temperatures are shown in Table I. The temperature dependent refined lattice parameters, oxygen occupancies and oxygen content are shown in Figs. 3(a) and 3(b). The refined oxygen content [inset in Fig. 3(b)] agrees within 1.6% with the value of 5.48 obtained by iodometric titration.

Our DSC measurement reveals a first transition at $T_{MI}=344$ K (Fig. 2, left), which corresponds to the previously reported metal-insulator (MI) transition.[5,6,9] At this temperature, our neutron diffraction measurements display a kink in the lattice parameters [Fig. 3(a)]. We also see a marked increase of the Co1-O7 distance and a simultaneous shrinking of the Co2-O7 distance [Figs. 3(c)–3(e)], which is responsible for the increased (decreased) volume of the octahedra (pyramids). This behavior has been reported before by Frontera *et al.*[6] for a $GdBaCo_2O_{5.5}$ powder sample investigated by ultrahigh resolution synchrotron radiation. This group associates the insulator to metal transition to a spin-state transition (low spin to high spin state) of the Co1 located in the octahedral environment. Since a Co^{3+} in higher spin state has a larger ionic radius, the volume of the octahedra has to increase. Due to the planes of octahedra along the *a* direction, expansion is easier in the *b* direction.

The DSC measurement shows a second transition at $T_{OD}=776$ K (Fig. 2, left). A typical NPD for $T=820$ K is shown in Fig. 4. In the NPD patterns one sees a merging of peaks across T_{OD} for which $k_2=2h_1$ (in orthorhombic notation), i.e., merging of (4 0 0) with (0 8 0), see inset in Fig. 4. As can be seen in Fig. 3(a), the values of the lattice parameters *a* and *b*/2 converge with increasing temperature, indicating that the symmetry evolves from orthorhombic to tetragonal. Indeed, above 780 K we obtain good refinements (Table I) using the tetragonal space group *P*4/*mmm* (unit

TABLE I. Structural parameters for $PrBaCo_2O_{5.48}$ ($\lambda=1.494$ Å): $T<T_{OD}$, refined in the *Pmmm* space group with sites: Ba 2*o* (0.5 y 0); Pr 2*p* (0.5 *y* 0.5); Co1 2*r* (0 0.5 *z*); Co2 2q (0 0 *z*); O1 1*a* (0 0 0); O2 1e (0 0.5 0); O3 1*g* (0 0.5 0.5); O4 1*c* (0 0 0.5); O5 2*s* (0.5 0 z); O6 2*t* (0.5 0.5 z); and O7 4*u* (0 y *z*). $T>T_{OD}$, refined in the *P*4/*mmm* space group with sites: Ba 1*c* (0.5 0.5 0); Pr 1*d* (0.5 0.5 0.5); Co 2*g* (0 0 *z*); O1 1*a* (0 0 0); O2 1*b* (0 0 0.5); and O3 4*i* (0 0.5 *z*).

Pmmm	300 K	375 K	600 K	750 K	775 K	780 K	*P*4/*mmm*	785 K	790 K	820 K
a (Å)	3.9068(1)	3.8978(1)	3.9104(1)	3.9284(1)	3.9353(1)	3.9381(1)	*a* (Å)	3.9525(1)	3.9536(1)	3.9554(1)
b (Å)	7.8807(1)	7.8981(1)	7.9316(1)	7.9408(1)	7.9354(2)	7.9318(2)				
c (Å)	7.6145(2)	7.6438(2)	7.6782(2)	7.7004(2)	7.7031(2)	7.7039(2)	*c* (Å)	7.7020(1)	7.7040(1)	7.7070(2)
Ba(*y*)	0.2508(15)	0.2515(15)	0.2545(13)	0.2512(16)	0.2476(19)	0.2456(21)				
Pr(*y*)	0.2670(15)	0.2675(20)	0.2624(16)	0.2657(21)	0.2675(23)	0.2682(23)				
Co1(*z*)	0.2524(18)	0.2509(24)	0.2523(20)	0.2537(26)	0.2510(30)	0.2502(32)	Co(*z*)	0.2514(10)	0.2504(09)	0.2516(13)
Co2(*z*)	0.2481(18)	0.2498(25)	0.2444(20)	0.2438(26)	0.2454(30)	0.2480(32)				
O5(*z*)	0.3055(11)	0.3048(13)	0.3043(11)	0.3034(14)	0.2991(19)	0.2973(23)	O3(*z*)	0.2872(03)	0.2867(02)	0.2867(04)
O6(*z*)	0.2669(14)	0.2653(17)	0.2645(13)	0.2766(13)	0.2791(18)	0.2816(21)				
O7(*y*)	0.2405(08)	0.2370(11)	0.2376(08)	0.2366(11)	0.2375(13)	0.2370(15)				
O7(*z*)	0.2836(09)	0.2864(10)	0.2870(08)	0.2824(10)	0.2826(12)	0.2838(13)				
Occ. O3	0.92(2)	0.86(3)	0.84(2)	0.73(4)	0.70(4)	0.52(5)	Occ. O2	0.51(2)	0.50(2)	0.49(2)
Occ. O4	0.06(1)	0.14(2)	0.14(2)	0.33(3)	0.37(4)	0.50(5)				
Ox. Cont.	5.49(1)	5.50(2)	5.49(2)	5.53(2)	5.54(3)	5.52(3)	Ox. Cont.	5.51(2)	5.50(2)	5.49(2)
χ^2	3.1	1.6	2.8	2.2	2.6	2.6	χ^2	2.8	2.9	1.5
R_{Bragg}	4.8	4.6	4.9	4.9	5.3	5.1	R_{Bragg}	4.7	4.6	6.0

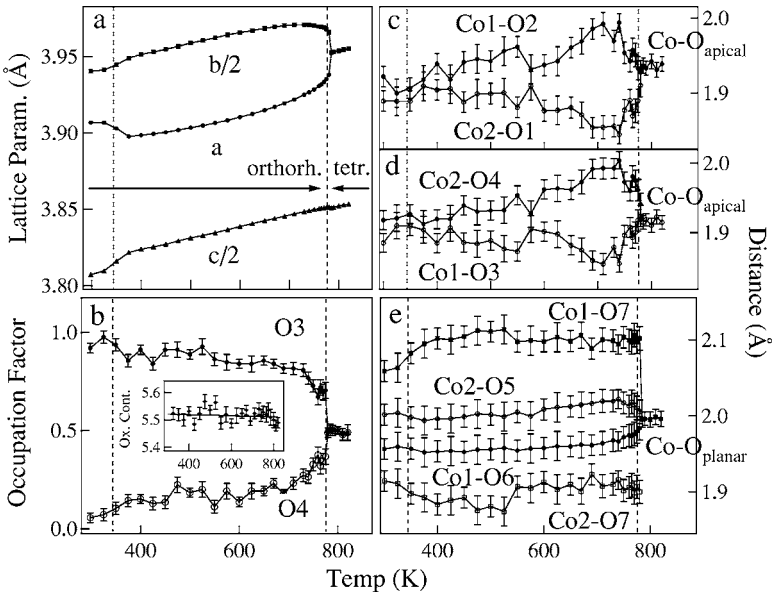

FIG. 3. Temperature evolution of (a) the lattice parameters; (b) the occupancy of the oxygen ion sites O3 and O4, inset: refined oxygen content; and (c), (d), (e) the Co-O distances (orthorhombic notation). Measured with $\lambda = 1.494$ Å. The vertical lines mark the positions of T_{MI} and T_{OD} as determined by DSC (see Fig. 2, left).

cell $a_p \times a_p \times 2a_p$). Additionally, we observe a redistribution of oxygen ions: the oxygen O4 occupancy increases at the expense of the O3 one, until the two sites display equivalent occupancies [see Figs. 1 and 3(b)]. No change of the occupancy of both planar and the other apical oxygen ions occurs across T_{OD}. This redistribution of oxygen leads to a disordered state in view of oxygen vancancies, since the planes of CoO_5 pyramids and CoO_6 octahedra no longer alternate along the b direction.

The metal-insulator and order-disorder transitions are reversible: a slight hysteresis effect is observed in the DSC measurement (Fig. 2, left), where the transition temperatures on cooling are by 3 K (T_{OD}) and 6 K (T_{MI}) lower than on heating. The temperature dependent evolution of the (0 8 0) and (4 0 0) reflections as determined by NPD ($\lambda = 1.889$ Å) is shown in Fig. 2, right. The material recovers its initial orthorhombic structure, only small modifications are seen in the diffractions patterns, which are due to the slightly different oxygen content. The oxygen content after the high temperature experiment lies between 5.56(1) (iodometric titration) and 5.46(6) (refinement of NPD data).

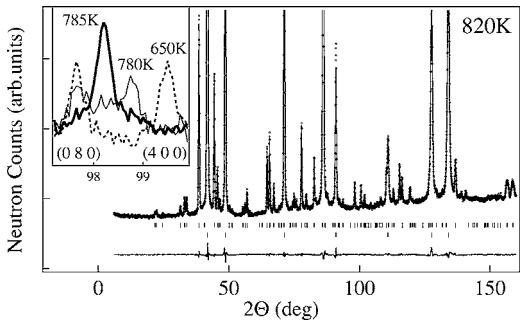

FIG. 4. Observed, calculated, and difference NPD pattern for $PrBaCo_2O_{5.48}$ at 820 K ($\lambda = 1.494$ Å). Peak positions are shown by ticks | (upper set from sample, lower one from steel container). The scale of the y axis is such that the steel reflections are cut. The inset shows merging of the (0 8 0) and (4 0 0) peaks (orthorhombic notation, $\lambda = 1.494$ Å) upon crossing T_{OD}.

We will now discuss our transport data. The drop in resistivity ρ at $T_{MI} = 344$ K and subsequent weak increase with temperature [Fig. 5(a)] seem to indicate metallic conductivity in $PrBaCo_2O_{5.48}$ above 344 K. However, the experimental value $\rho \sim 1200$ $\mu\Omega$ cm above T_{MI} ($\rho_{ab} \sim 600$ $\mu\Omega$ cm according to single crystal measurements by Taskin *et al.*[27]) is still higher than the resistivity of many 3*d*-metal oxides.[19] Furthermore, the temperature dependence of the resistivity in $PrBaCo_2O_{5.48}$ does not show a simple metallic behavior. The observed weak temperature dependence of $\rho(T)$ above T_{MI} can be explained in terms of a temperature-activated Arrhenius-type mobility, namely small polaron conduction, similar to that proposed for $La_{1-x}Sr_xCoO_3$ (Ref. 19) and $Ca_2Co_{0.8}Ga_{0.2}O_{4.8}$.[28] The positive sign of the thermoelectric power S [Fig. 5(b)] is an indication that holes are the majority charge carriers.[28] Hole-conductivity in cobaltites is usually related to the presence of Co^{4+} ions[29] and, as in other perovskite systems,[28–30] the thermally induced charge disproportionation reaction $2Co^{3+} \rightarrow Co^{2+} + Co^{4+}$ provides the Co^{4+} charge carriers. In our compound, following the positive sign of the thermopower S [Fig. 5(b)], the small polaron conduction mechanism incorporates mobile Co^{4+} holes, while electrons are trapped on Co^{2+} sites. From crystallographic considerations, Co^{2+} are probably located at the pyramidal sites, whereas the Co^{3+} and Co^{4+} are at the octahedral sites. The polaronic hopping conductivity is given by

$$\sigma = |e|\mu p = |e|p\frac{\mu_0}{T}\exp\left\{-\frac{E_a}{k_B T}\right\}, \qquad (1)$$

where E_a is the mobility activation energy, and μ and p represent mobility and volume concentration of holes (Co^{4+}), respectively.[31] Usually, $\exp\{-E_a/k_BT\}$ dominates and conductivity $\sigma(T)$ increases with temperature. However, an opposite temperature dependence of $\sigma(T)$ can be observed for low activation energies E_a.

As follows from Eq. (1) $\log \sigma T$ vs $1/T$ enables estimation of E_a [Arrhenius plot, shown in Fig. 5(b)]. A nearly constant activation energy $E_a \sim 0.04$ eV was obtained from these plots

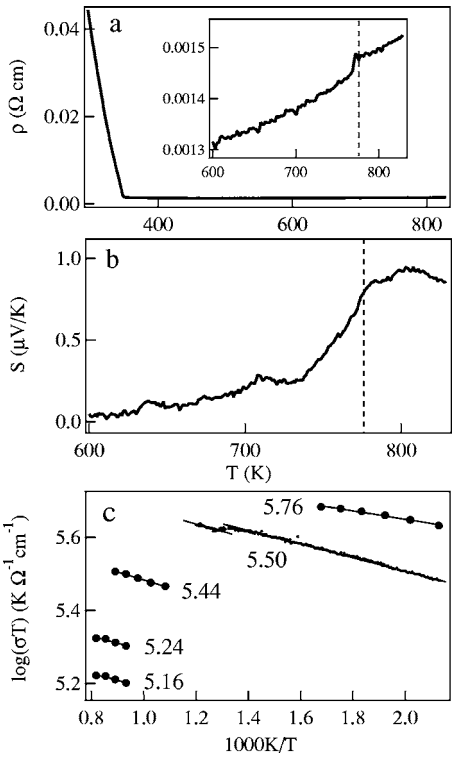

FIG. 5. Temperature dependence of the (a) dc resistivity ρ of $PrBaCo_2O_{5.50}$; (b) thermoelectric power S of $PrBaCo_2O_{5.50}$; and (c) Arrhenius line for $PrBaCo_2O_{5+\delta}$ (δ=0.16, 0.24, 0.44, 0.50, and 0.76).

independently of the oxygen content over the wide range of $0.16 \leqslant \delta \leqslant 0.50$ involved in the analysis. Importantly, the $\delta \leqslant 0.4$ $PrBaCo_2O_{5+\delta}$ compounds are reported to be semiconductors and do not exhibit a *MI* transition.[32] Consequently, the low resistivity at high temperatures as well as the weak $\rho(T)$ dependence are more consistent with a temperature-activated hole mobility than with metallic conductivity. The obtained low value of $E_a \sim 0.04$ eV is not exceptional for three-dimensional perovskites. An activation energy of $E_a \sim 0.15$ eV was found in the Ruddlesden-Popper ferrites $Sr_3Fe_2O_{6-\delta}$,[33] which exhibit a quasi-two-dimensional conductivity in theFeO_2 planes. A very small value of $E_a \sim 0.08$ eV was recently reported for $La_{0.4}Sr_{0.6}CoO_{3-\delta}$.[19]

The anomalies in the temperature behavior of both conductivity $\sigma(T)$ and thermoelectric power $S(T)$ [Figs. 5(a) and 5(c) across the phase transition at T_{OD}=776 K can be explained by a decrease of the charge carrier (hole) concentration p. Oxygen disorder above T_{OD} breaks an ideal alternation of octahedral and pyramidal planes, hampering the hole creation. It follows from Eq. (1) that a reduction of p results in a decrease of σ. On the other hand, according to the equation for thermopower

$$S = \frac{k_B}{|e|} \ln \frac{1-p}{p}, \tag{2}$$

a decrease of hole concentration should cause an increase of S. Both effects have been observed in our measurements [see Figs. 5(a) and 5(c)].

The oxygen disorder above T_{OD} can also favor ionic conductivity due to random redistribution of the structural vacancies over the O3 and O4 positions, as shown for certain perovskite systems.[15–19,33] A similar effect was found in layered ferrites $Sr_3Fe_2O_{6-\delta}$, where disordering of the FeO_5 pyramides results in a rapid increase of the ionic conductivity.[33] Further studies of the ionic conductivity are necessary to clarify this issue.

To conclude, we have investigated $PrBaCo_2O_{5.48}$ in the temperature range 300 K$\leqslant T \leqslant$820 K and found a transition at T_{OD}=776 K which is accompanied by an increase of the crystallographic symmetry from orthorhombic *Pmmm* to tetragonal *P*4/*mmm*. Due to the redistribution of oxygen vacancies the compound goes from an ordered to a disordered state, breaking down the alternation of CoO_5 pyramidal and CoO_6 octahedral planes. Our conductivity measurements on $PrBaCo_2O_{5.48}$ provide evidence for a semiconducting (instead of metallic) state above T_{MI}. The activation energy of conductivity is comparable to that of semiconducting $PrBaCo_2O_{5+\delta}$ ($\delta \leqslant 0.44$) and suggests a temperature activated hole (polaronic) mobility. The oxygen vacancy disorder above T_{OD} reduces hole conductivity, due to the loss of an ideal alternation of CoO_5 pyramidal and CoO_6 octahedral planes along the *b* direction.

The experiments were partly performed at the Swiss Spallation Neutron Source SINQ, PSI Villigen, Switzerland. This work was supported by the Russian Foundation for Basic Research Grant No. 04-03-32948a and by the Swiss National Science Foundation through SCOPES IB7320-110859/1, Marie Heim-Voegtlin No. PMPD2-111324/1, and NCCR MaNEP project.

*Electronic address: Sabine.Streule@psi.ch

[1] J. B. Goodenough, Mater. Res. Bull. **6**, 967 (1971).
[2] M. A. Señarís-Rodríguez and J. B. Goodenough, J. Solid State Chem. **116**, 224 (1985).
[3] T. Vogt, J. A. Hriljac, N. C. Hyatt, and P. Woodward, Phys. Rev. B **67**, 140401(R) (2003).
[4] I. O. Troyanchuk, N. V. Kasper, D. D. Khalyavin, H. Szymczak, R. Szymczak, and M. Baran, Phys. Rev. Lett. **80**, 3380 (1998).
[5] A. Maignan, C. Martin, D. Pelloquin, N. Nguyen, and B. Raveau, J. Solid State Chem. **142**, 247 (1999).
[6] C. Frontera, J. L. García-Muñoz, A. Llobet, and M. A. G. Aranda, Phys. Rev. B **65**, 180405(R) (2002).
[7] T. Vogt, P. M. Woodward, P. Karen, B. A. Hunter, P. Henning, and A. R. Moodenbaugh, Phys. Rev. Lett. **84**, 2969 (2000).
[8] E. Suard, F. Fauth, V. Caignaert, I. Mirebeau, and G. Baldinozzi, Phys. Rev. B **61**, R11871 (2000).
[9] F. Fauth, E. Suard, V. Caignaert, B. Domengès, I. Mirebeau, and L. Keller, Eur. Phys. J. B **21**, 163 (2001).

[10] C. Martin, A. Maignan, D. Pelloquin, N. Nguyen, and B. Raveau, Appl. Phys. Lett. **71**, 1421 (1997).
[11] D. D. Khalyavin, S. N. Barilo, S. V. Shiryaev, G. L. Bychkov, I. O. Troyanchuk, A. Furrer, P. Allenspach, H. Szymczak, and R. Szymczak, Phys. Rev. B **67**, 214421 (2003).
[12] A. A. Taskin, A. N. Lavrov, and Y. Ando, Phys. Rev. Lett. **90**, 227201 (2003).
[13] Y. Moritomo, T. Akimoto, M. Takeo, A. Machida, E. Nishibori, M. Takata, M. Sakata, K. Ohoyama, and A. Nakamura, Phys. Rev. B **61**, R13325 (2000).
[14] Y. Teraoka, H. M. Zhang, N. Furukawa, and N. Yamazoe, Chem. Lett. **11**, 21743 (1985); Y. Teraoka, T. Nobunaga, K. Okamoto, N. Miura, and N. Yamazoe, Solid State Ionics **48**, 207 (1991).
[15] H. Kruidhof, H. J. M. Bouwmeester, R. H. E. van Doorn, and A. J. Burggraaf, Solid State Ionics **63-65**, 816 (1993).
[16] R. H. E. van Doorn and A. J. Burggraaf, Solid State Ionics **128**, 65 (2000).
[17] S. Adler, S. Russek, J. Reimer, M. Fendorf, A. Stacy, Q. Huang, A. Santoro, J. Lynn, J. Baltisberger, and U. Werner, Solid State Ionics **68**, 193 (1994).
[18] M. V. Patrakeev, I. A. Leonidov, E. B. Mitberg, A. A. Lakhtin, V. G. Vasiliev, V. L. Koshevnikov, and K. R. Poeppelmeier, Ionics **5**, 444 (1999).
[19] E. B. Mitberg, M. V. Patrakeev, I. A. Leonidov, V. L. Kozhevnikov, and K. R. Poeppelmeier, Solid State Ionics **130**, 325 (2000).
[20] S. Streule, A. Podlesnyak, J. Mesot, M. Medarde, K. Conder, E. Pomjakushina, E. Mitberg, and V. L. Kozhevnikov, J. Phys.: Condens. Matter **17**, 3317 (2005).
[21] K. Conder, E. Pomjakushina, A. Soldatov, and E. B. Mitberg, Mater. Res. Bull. **40**, 257 (2005).
[22] M. V. Patrakeev, I. A. Leonidov, V. L. Kozhevnikov, and K. R. Poeppelmeier, J. Solid State Chem. **178**, 921 (2005).
[23] M. V. Patrakeev, E. B. Mitberg, A. A. Lakhtin, I. A. Leonidov, V. L. Kozhevnikov, and K. R. Poeppelmeier, Ionics **4**, 191 (1998).
[24] P. Fischer, G. Frey, M. Koch, M. Könnecke, V. Pomjakushin, J. Schefer, R. Thut, N. Schlumpf, R. Bürge, U. Greuter, S. Bondt, and E. Berruyer, Physica B **276**, 146 (2000).
[25] J. Rodríguez-Carvajal, Physica B **192**, 55 (1993).
[26] M. Respaud, C. Frontera, J. L. García-Muñoz, M. Á. G. Aranda, B. Raquet, J. M. Broto, H. Rakoto, M. Goiran, A. Llobet, and J. Rodríguez-Carvajal, Phys. Rev. B **64**, 214401 (2001).
[27] A. A. Taskin and Y. Ando, Phys. Rev. Lett. **95**, 176603 (2005).
[28] S. Y. Istomin, E. V. Antipov, G. Svensson, J. P. Attfield, V. L. Kozhevnikov, I. A. Leonidov, M. V. Patrakeev, and E. B. Mitberg, J. Solid State Chem. **167**, 196 (2002).
[29] S. R. Sehlin, H. U. Anderson, and D. M. Sparlin, Phys. Rev. B **52**, 11681 (1995).
[30] M. V. Patrakeev, I. A. Leonidov, and V. L. Kozhevnikov, Solid State Ionics **82**, 5 (1995).
[31] H. L. Tuller, in *Ceramic Materials for Electronics*, edited by R. C. Buchanan (Dekker, New York, 1986), p. 425.
[32] A. A. Taskin, A. N. Lavrov, and Y. Ando, Phys. Rev. B **71**, 134414 (2005).
[33] Y. A. Shilova, M. V. Patrakeev, E. B. Mitberg, I. A. Leonidov, V. L. Kozhevnikov, and K. R. Poeppelmeier, J. Solid State Chem. **168**, 275 (2002).